

PCCP

Accepted Manuscript



This is an *Accepted Manuscript*, which has been through the Royal Society of Chemistry peer review process and has been accepted for publication.

Accepted Manuscripts are published online shortly after acceptance, before technical editing, formatting and proof reading. Using this free service, authors can make their results available to the community, in citable form, before we publish the edited article. We will replace this *Accepted Manuscript* with the edited and formatted *Advance Article* as soon as it is available.

You can find more information about *Accepted Manuscripts* in the [Information for Authors](#).

Please note that technical editing may introduce minor changes to the text and/or graphics, which may alter content. The journal's standard [Terms & Conditions](#) and the [Ethical guidelines](#) still apply. In no event shall the Royal Society of Chemistry be held responsible for any errors or omissions in this *Accepted Manuscript* or any consequences arising from the use of any information it contains.



Journal Name

COMMUNICATION

Observation of the retarded transportation of the photogenic hole on the epitaxial graphene

Received 00th January 20xx,
Accepted 00th January 20xx

Shujie Wang, Xizhi Yuan, Xiaofeng Bi, Xiaomei Wang, Qingsong Huang*

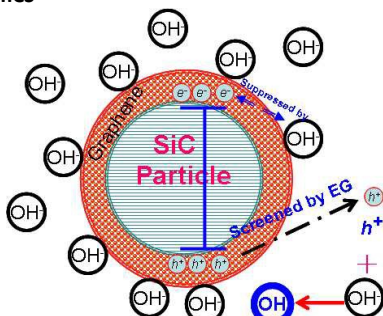
DOI: 10.1039/x0xx00000x

www.rsc.org/

ABSTRACT

Graphene is usually adopted as the assistant additives of catalysts in photocatalysis process, because of its ability in accelerating separation of photogenic charge carriers. To elucidate the mechanism, the hydrogen peroxide is adopted to change the $O_2^{\cdot-}$ active species into the OH^{\cdot} towards degradation of the organic dye. If the PH value is less than 7, the concentration of the OH^{\cdot} species can be reduced more quickly with the additive of graphene than without, because the negative charged electrons can be transported quickly on graphene. If the PH value is larger than 7, the concentration of OH^{\cdot} can be promoted by the catalyst SiC with the photogenic h^+ releasing and reacting with the OH^{\cdot} , however is reduced if covered by graphene sheet, retarding the h^+ releasing from SiC substrate. Our findings have provided a certification of role of graphene in photo-catalysis process.

TOC GRAPHICS



In the alkaline resolutions, the epitaxial graphene retards the transportation of the photogenic hole from SiC substrate.

KEYWORDS

Photo-generated Charge Carrier, SiC Particle, Graphene Sheet on SiC, Pollutant Degradation, Organic Dye, Active Species of Catalysis

Since the graphene discovery,¹ it has been studied and applied

widely in many fields,²⁻⁷ such as the organic photovoltaics,⁸⁻¹¹ the batteries,¹² the transistors,¹³ the biology,¹⁴ the hydrogen storage,¹⁵ and the field-emission cathodes,^{16,17} etc. The enhancement of the photo-catalysis is one of the applications.¹⁸⁻²¹ Since its high charge carrier mobility and ballistic transportation,^{22,23} graphene is adopted to accelerate the separation of the photogenic charge carriers. Usually, the graphene oxide (GO) is prepared by the modified Hummers method. The graphene is reduced from the GO, and mixed with catalyst nano-particles, such as TiO_2 ,^{24,25} ZnO ,^{26,27} CdS ,²⁸ CuS ,²⁹ C_3N_4 ,³⁰ gold particles³¹ and SiC ¹⁹ etc. Because of the limitation of the preparation method, the performance of the graphene is restricted and can not display its intrinsic properties fully. When the nano-particles are decorated on the network of the graphene sheet, their photo-catalysis performances are enhanced significantly. Many works^{18,19,32} point out that the graphene has played an important role in the separation of the photo-generated charge carrier (SPGC), because of its ballistic transportation, including both of the electron and the hole.^{22,23} However, no direct evidence is observed by now to elucidate the mechanism of separation process, no more than further evidence to enhance the transportation of the photogenic electron by retarding that of the hole on the graphene sheet. To such end, a simple experiment should be designed to confirm the role of graphene in the photo-catalysis process. In the experiment, the photogenic charge carriers, electron transportation can be accelerated, and on the contrary, the transportation of hole can be selectively prevented by the graphene sheet.

In this letter, a degradation of organic substance, Rhodamine B (RhB), by hydrogen peroxides conforms to the requirement and is presented to demonstrate the enhanced SPGC by the graphene sheet. When the hydrogen peroxides are resolved in water, and their concentration is controlled within a scope, part of them will change to active species, OH^{\cdot} (ASH), and reach a balance finally. The balance constant can be marked as k , depending on the concentration, the light irradiation and temperature mainly. As a result, the concentration of the ASH species determines the photo-catalysis ability. Irradiated by the ultraviolet (UV) light, the k value can be promoted to a higher level, and the concentration of the ASH increases as well. The excited RhB dye molecules release

School of Chemical Engineering, Sichuan University, Chengdu 610065, China

*Corresponding author

E-mail address: qshuang@scu.edu.cn

DOI: 10.1039/x0xx00000x

electrons, which can be absorbed by ASH and become OH^\cdot , and lose its catalytic activity. Here, the SiC powder is introduced into the solution, some electrons can be excited from valance band to conductance band by the UV light irradiation. The excited electrons will also transfer to the ASH and lower down its concentration, so that the degradation rate of the RhB molecular decreases correspondingly. With introduction of the graphene sheets, and the PH value less than 7, the lowered degradation performance discloses that the graphene sheet on SiC (GSSC) can accelerate the transportation of the excited electrons, and reduce the concentration of the ASH species more quickly than the bare SiC powder. Interestingly, when the PH is larger than 7, the concentration of the ASH species can be increased by the bare SiC and the corresponding GSSC, where the photogenic hole can be released and reacts with OH^\cdot into ASH. A lower photo-catalysis performance of the GSSC with respect to the bare SiC is observed, because the photogenic hole suffers the screening effect of the graphene, where only part of the holes can penetrate the graphene film.

The GSSC particles can be prepared by a thermal annealing technique at 1100°C and under 0.2 atmosphere pressures for 30 minutes. A scanning electron microscopy (SEM) image reveals that the GSSC is completely covered by the transparent graphene film, and the size is around $30\ \mu\text{m} \pm 10\ \mu\text{m}$ (Fig. 1a). The surface graphene can be peeled off by the conductive resin (Fig. 1b), displaying some cotton-like structures. Meanwhile, such kind of graphene structure can be striped by the sonication chemical method, by which the cotton-like graphene plates are collected and characterized by a transmission electron microscopy (TEM) (Fig. 1c). A Raman scattering was performed to check the GSSC structure, the spectrum reveals that the graphene on the surface is composed of the graphene nanoplates (GN) with size in 100 nm order of magnitude (Fig. 1d). Furthermore, the graphene film on the SiC surface looks connected each other and the charge carriers can be transported to any of the GN nanoplates. All the synthesis and characterization methods refer to the Experimental Section in Supporting Information (ESI). The substrate SiC is the 6H-SiC powders (Sigma, Inc.), which can be verified by the X-ray diffraction (XRD) spectrum. The initial concentration of RhB molecules is around 1.67×10^{-2} mM, and the concentration of the hydrogen peroxide is selected as 58.7 mM. The XRD spectrum (Fig. 1e red line) refers to the standard 6H-SiC (Card No. #29-1128), which is inconsistent with our substrate SiC samples (Fig. 1e blue line). The green line displays the GSSC characteristics, where the epitaxial graphene can be identified as the plum peak around $21.95^\circ(2\theta)$, and clarified by an enlarged black line. The peak position reveals that the inter-distance between the adjacent layers is around 0.40558 nm, suggesting the coupling force between the adjacent graphene sheets is much weaker than that of graphite in AB stacking with interlayer distance around 0.335nm, so that the GSSC can be regarded as the quasi-freestanding graphene.^{33,34}

Before the degradation of the RhB dye by a hydrogen peroxide, a direct photocatalysis by the SiC particles and the SiC/graphene composite is performed to evaluate the influence of active species $\text{O}_2^{\cdot-}$ (ASO), which can be inferred from the Fig. 2a and Fig. S1, where the low level of the ASO makes the degradation time of RhB irradiated by UV light more than 2 hours. Because of the

long time irradiation, the photosensitization process of RhB can be observed absolutely (Fig. 2a pink line). Under the UV light irradiation, the excited RhB molecule can release the electrons, collected by the resolved O_2 to form the ASO species. As a result, the excited SiC can release the photogenic electrons in the dionized water with a weak acid environment (PH=6), and the concentration of the ASO species increases as well correspondingly, in consistent with the trench of the red line. When the graphene epitaxially grows on the surface of

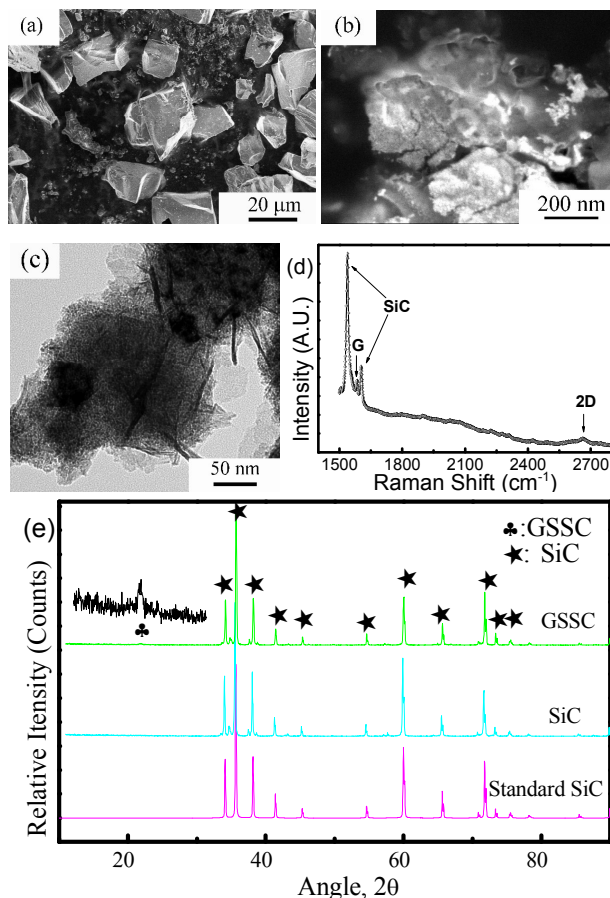


Figure 1 Epitaxial growth Graphene sheet (EG) on the silicon carbide (SiC) particle surface at temperature of 1120°C for 90 minutes. (a) SEM image, (b) SEM image of the EG exfoliated from SiC particles, (c) TEM image of exfoliated graphene from SiC particles, (d) The Raman spectrum, (e) The XRD spectra revealing the epitaxial graphene on 6H-SiC substrate.

the SiC as GSSC particle, it transports the photogenic electrons from the SiC, and the concentration of the ASO species increase further (Fig. 2a green line). Some freestanding graphene powder has been prepared via Hummer method to the reduction of graphene oxide (rGO) (Fig. 2b). Because the rGO powder is composed of the nanoflakes, its Raman spectrum displays high D peak and low 2D peak with a large full width of half maximum (FWHM) (Fig. 2c). With such rGO powder, the photosensitization of RhB molecules can be accelerated, since the photogenic electrons are transferred to form ASO species. It seems the releasing of electrons by photosensitization process is more easily than that by the photocatalysis process on the SiC surface (Violet line). If the rGO sheets

are coated on the SiC particles, part of the rGO is released to the deionized water towards the photosensitization process, while the left rGO enwrapped on the SiC particles enhances the photocatalysis of the SiC particle. The electrons both from the SiC surface and the RhB molecules can be accelerated to form ASO species (Fig. 2a blue line), enhancing the degradation performance.

With the irradiation of the UV light, the additive of hydrogen peroxides in the resolution can change the active species from the ASO to the ASH. Upon the pH around 6, the photogenic electron is the major species, transporting on the surface of graphene (Fig. 2d and Fig. S2). As the evidence of Fig. 2d and Fig. S3a, the photosensitization of RhB under UV irradiation shows no degradation effect in five minutes, and the same phenomenon can be observed upon the degradation of the RhB under dark field, revealing no photosensitization and the related electron transformation. The irradiation of UV light activates the degradation of the hydrogen peroxide (Fig. 2d rectangle black line). In principal, the rGO can enhance the transportation of the electrons from the excited RhB molecules by the UV light to the ASH, which reduces the concentration of the ASH species (Fig. 2d purple line). Furthermore, the additive of SiC micro-particles can introduce the excited electrons to their conductive band (CB), which can also reduce the concentration of the ASH species, offering the reduced degradation ability even weaker than that by the rGO flakes (Fig. 2d red line). When the GSSC is applied (Fig. 2d green line), the worst degradation performance suggests the lowest concentration of ASH in the all catalysts, since the surface graphene on the SiC can accelerate the electrons to transfer from the SiC particle to the ASH. In general, when the photogenic electrons are active species, they can be accelerated to move along the graphene film and to reduce the concentration of the ASH species, leading to a worse degradation performance of the dye than the bare SiC.

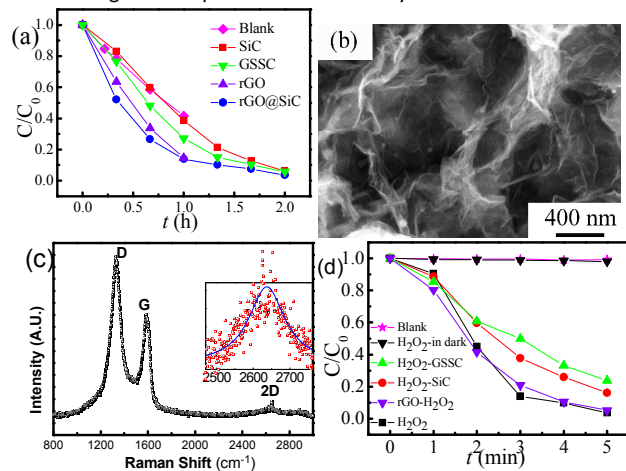


Figure 2 Photo-degradation of RhB without the hydrogen peroxide (a), and the SEM image of the rGO (b), and the rGO Raman spectrum (c), suggesting a high crystallized graphene film. (d) The photo-degradation of RhB by the hydrogen peroxide with PH=6.

To activate the charge electron or hole alternatively, the different PH values are selected during the photo-degradation process with the hydrogen peroxide. With tuning the PH value to 1, the positive charged H^+ ions suppress the same charge photogenic carrier hole (h^+), and activate the negative photogenic electrons. The rich H^+ ions can further remove away any negative charged carriers, offering an efficient environment towards an exotic quick

degradation performance (Fig. 3a). Since the electrons can be captured by the H^+ ions, the ASH concentration can be kept from reducing significantly by the photogenic electrons, offering a very quick degradation rate as well (Fig. 3b). When the micro-sized SiC powder is adopted, the photo-generated electrons from excited SiC will partly transfer to the ASH species, decreasing the concentration of the ASH and the degradation rate. Furthermore, the GSSC degradation line reveals that the graphene film has favoured the photogenic electrons to move to the ASH, displaying the even lowest degradation rate in Fig. 3a. To avoid the possible influence of the overdosage of the hydrogen peroxide with a high concentration,²⁴ a diluted hydrogen peroxide (ca. 0.0001 times) is adopted to perform the same degradation process (Fig. 3b). By adopting the Langmuir-Hinshelwood model,³⁵ a photo-degradation kinetic plot of the degradation dye has been presented in the Fig. S3b through Fig. S3b', and the same results as Fig. 3b can be obtained. Both of the Fig. S3b and Fig. S3b' can be used to evaluate the degradation rate of the dye. The Fig. S3b' is normally adopted to estimate the average degradation rate by a straight line fit of the related points. Since the concentration of the hydrogen peroxide is reduced sharply, the concentration of the ASH species is lowered down correspondingly. As a result, the degradation performance is worsened and the degradation time is prolonged (Fig. 3b). Figure 3c illustrates the possible transportation routes of the photogenic electrons. Most of the photogenic electrons are captured by the H^+ ions, while a small part of them can reach the ASH. The concentration of the ASH can be sustained accordingly, which can attribute the high quick degradation performance of the dye RhB.

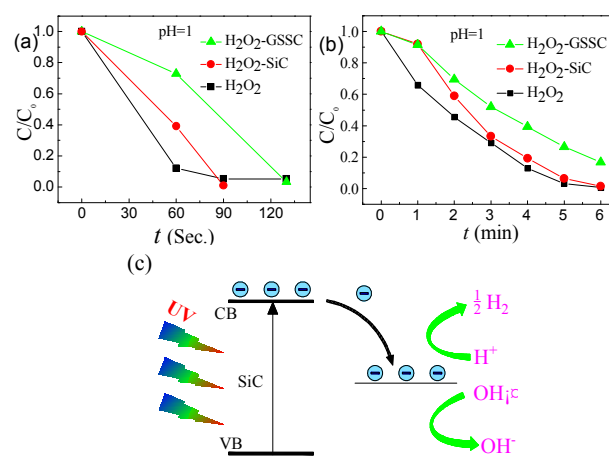


Figure 3 The degradation performance of the RhB when the PH value equals 1. The photo-catalysis process with additive of (a) high concentration of hydrogen peroxide and (b) The diluted hydrogen peroxide. (c) The schematic for the possible transformation path of photogenic electron.

When the PH value is tuned to 12 with additives of the hydrogen peroxide (Fig. 4a-b black line), the negative charged OH^- ions and the activated RhB can suppress the same charge photogenic electrons (e^-), and activate the positive photogenic holes. As a result, the extra OH^- ions can capture any photogenic holes, and the concentration of the ASH can be increased. When the SiC powder is adopted, the photogenic carrier hole (h^+) reacts with the OH^- ions

and forms the ASH, offering a higher concentration of ASH, and increase the degradation performance of RhB molecules (Fig. 4a-b red line). Interestingly, when the graphene epitaxially grows on the SiC surface, the photogenic carrier hole (h^+) becomes difficult to leave the surface of the SiC and penetrate the graphene film to reach the OH^- ions (Fig. 4a-b green line). The same kinetic plots of degradation RhB are displayed by using the Langmuir-Hinshelwood model (Fig. S3c and Fig. S3c'). The leakage from the boundaries of graphene plates should be neglected, referring to the Fig. S4. As shown in Fig. S4a, the degradation process of the dye RhB was performed in a resolution of the hydrogen peroxide by the irradiation of visible light ($\lambda > 400$ nm), which can be slowed down by the additives of the SiC powders, and the performance can be restored by the epitaxial graphene, which means the SiC particles are wrapped tightly without leakage. The same phenomenon was also observed when the PH value was 12 (Fig. S4b).

The photogenic holes from the SiC can be screened by the epitaxial graphene, and only part of them can penetrate the epitaxial graphene to reach the negative charged OH^- ions (Fig. 4c). Thus the concentration of the ASH species is lower than that of the bare SiC powder (Fig. 4b), but higher than that of the hydrogen peroxide only (Fig. 4b). The screening (retarding) effect cannot be ascribed to the scatter of the topological defects on the epitaxial graphene, and the structure of the epitaxial graphene film, otherwise, the electron also can be scattered by the defects and structures. Meanwhile, the retarding effects cannot be ascribed to the low chemical potential as well,^{23,24,36,37} because the bare SiC can release hole even more effectively. Thus, the retarding effects can only be attributed to the intrinsic properties of epitaxial graphene in alkali resolution. Although some works have mentioned the GO and rGO behave like a good hole transport layer in solar cell, it only represents that even retarded graphene also display a better performance than some conducting polymers.^{38,39}

A photo-catalysis of the dye RhB is also performed with the diluted hydrogen peroxide (ca. 0.0001 times), a same phenomenon is also observed (Fig. 4b). Since the concentration of the hydrogen peroxide was diluted, the corresponding concentration of the ASH species was also decreased, suggesting a lower degradation performance.

In addition, since the dye RhB is very easy to be excited to release electrons by the UV-vis light,⁴⁰⁻⁴² it should have influence on the release of the photogenic electrons. Here, the concentration of dye have been tuned to the double (Fig. 4d) and the half (Fig. 4e) of the original one (1.67×10^{-2} mM) to perform the retarding effect of the graphene. With the concentration of hydrogen peroxide is diluted to its 0.0001 fold ($C_{\text{H}_2\text{O}_2} = 5.87 \times 10^{-6}$ M), the retarding effect can be reappeared strictly (Fig. 4d-e). Furthermore, without the dilution of the hydrogen peroxide, the effects of the dye RhB on the retarding effect are displayed in Fig. S5. When the concentration of the RhB is reduced to half of the original one (1.67×10^{-2} mM), for the bare SiC particles, the OH^- anions and the dye RhB can suppress the releasing of the photogenic electrons of the SiC effectively (Fig. S5a), however the epitaxial graphene on GSSC can enhance the releasing of the photogenic electrons, and retarding the transportation of the photogenic holes of the substrate SiC. Thus, the photo-degradation rate of the GSSC can be even slower than that of the hydrogen peroxide only (Fig. S5b).

When the PH value is 1, the degradation product can be removed by the H^+ ions, whereas the concentration of the product can not be reduced by the OH^- ions when the PH value is 12. A quicker degradation performance of the dye can be observed in Fig. 3 more than Fig. 4.

In summary, with the hydrogen peroxide adopted, the transportation of the negative charged electrons on graphene is enhanced with the PH less than 7. However, the retarded transportation of the positive charged photogenic hole on graphene is also observed with the PH value more than 7. Even a more diluted solution is adopted, the same result is obtained. Our findings have opened a facile way to observe the carrier transportation in the different semiconductor.

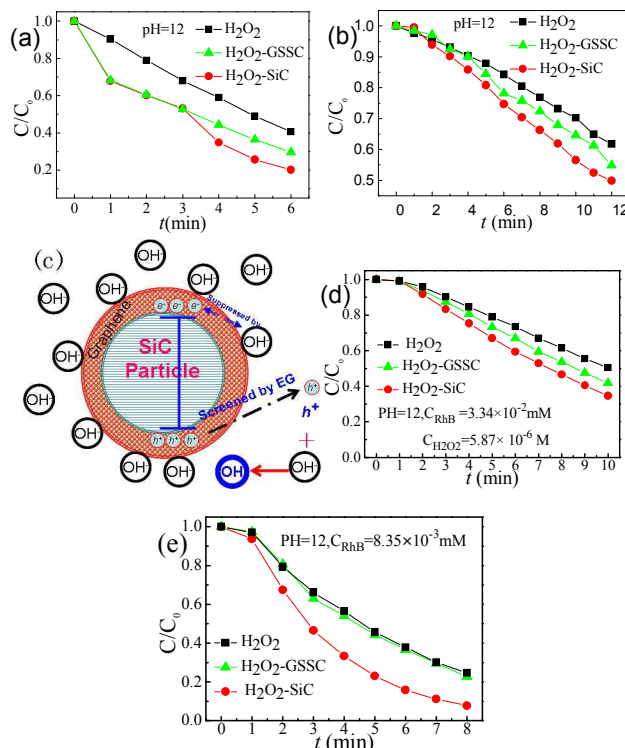


Figure 4 The degradation process is performed when PH value equals 12. The photo-catalysis process with additive of (a) high concentration of hydrogen peroxide ($C_{\text{H}_2\text{O}_2} = 58.7$ mM, and $C_{\text{RhB}} = 1.67 \times 10^{-2}$ mM) and (b) The low concentration of hydrogen peroxide ($C_{\text{H}_2\text{O}_2} = 5.87 \times 10^{-6}$ M, and $C_{\text{RhB}} = 1.67 \times 10^{-2}$ mM). (c) The schematic for the possible transformation path of photogenic electron. (d) The double concentration of RhB ($C_{\text{RhB}} = 3.34 \times 10^{-2}$ mM, and $C_{\text{H}_2\text{O}_2} = 5.87 \times 10^{-6}$ M). (e) The half concentration of RhB ($C_{\text{RhB}} = 8.35 \times 10^{-3}$ mM, and $C_{\text{H}_2\text{O}_2} = 5.87 \times 10^{-6}$ M).

Notes and references

† The authors declare no competing financial interests.

This work is supported partly by the National Natural Science Foundation of China (No. 51472170).

- 1 A. K. Geim, *Science*, 2009, **324**, 1530.
- 2 D. Chen, L. Tang, J. Li, *Chem Soc Rev*, 2010, **39**, 3157.
- 3 G. C. Xie, K. Zhang, B. D. Guo, Q. Liu, L. Fang, J. R. Gong, *Adv Mater*, 2013, **25**, 3820.
- 4 X. Li, W. Cai, J. An, S. Kim, J. Nah, D.; Yang, R. Piner, A. Velamakanni, I. Jung, E. Tutuc, S. K. Banerjee, L. Colombo, R. S. Ruoff, *Science*, 2009, **324**, 1312.
- 5 T. Xian, H. Yang, Y. F. Wang, L. J. Di, J. L. Jiang, R. S. Li, W. J. Feng, *Mater Trans*, 2014, **55**, 245.
- 6 S. Guo, S. Dong, *Chem Soc Rev*, 2011, **40**, 2644.
- 7 M. Pumera, *Chem Soc Rev*, 2010, **39**, 4146.
- 8 E. Stratakis, K. Savva, D. Konios, C. Petridis, E. Kymakis, *Nanoscale*, 2014, **6**, 6925.
- 9 G. Kakavelakis, D. Konios, E. Stratakis, E. Kymakis, *Chem Mater*, 2014, **26**, 5988.
- 10 D. Konios, C. Petridis, G. Kakavelakis, M. Sygletou, K. Savva, E. Stratakis, E. Kymakis, *Adv Funct Mater*, 2015, **25**, 2213.
- 11 N. Balis, D. Konios, E. Stratakis, E. Kymakis, *ChemNanoMat*, 2015, 10.1002/cnma.201500044.
- 12 J. Hassoun, F. Bonaccorso, M. Agostini, M. Angelucci, M. G. Betti, R. Cingolani, M. Gemmi, C. Mariani, S. Panero, V. Pellegrini, B. Scrosati, *Nano Lett*, 2014, **14**, 4901.
- 13 K. S. Novoselov, A. K. Geim, S. V. Morozov, D. Jiang, M. I. Katsnelson, I. V. Grigorieva, S. V. Dubonos, A. A. Firsov, *Nature*, 2005, **438**, 197.
- 14 C. K. Y. K. Chung, D. Shin, S. R. RYOO, B. H. Hong, D. H. Min Acc., *Chem. Res.*, 2013, **46**, 2211.
- 15 V. Tozzini, V. Pellegrini, *Phys. Chem. Chem. Phys.*, 2013, **15**, 80.
- 16 G. Viskadourous, D. Konios, E. Kymakis, E. Stratakis, *Appl Phys Lett*, 2014, **105**, 203104.
- 17 Q. S. Huang, G. Wang, L. W. Guo, Y. P. Jia, J. J. Lin, K. Li, W. J. Wang, X. L. Chen, *Small*, 2011, **7**, 450.
- 18 W. Lu, L. W. Guo, Y. P. Jia, Y. Guo, Z. L. Li, J. J. Lin, J. A. Huang, W. J. Wang, *Rsc Adv*, 2014, **4**, 46771.
- 19 K. X. Zhu, L. W. Guo, J. J. Lin, W. C. Hao, J. Shang, Y. P. Jia, L. L. Chen, S. F. Jin, W. J. Wang, X. L. Chen, *Appl Phys Lett*, 2012, **100**.023113.
- 20 X. F. Zhou, Q. Z. Gao, X. Li, Y. J. Liu, S. S. Zhang, Y. P. Fang, J. Li, *J Mater Chem A*, 2015, **3**, 10999.
- 21 W. G. Tu, Y. Zhou, Z. G. Zou, *Adv Funct Mater*, 2013, **23**, 4996.
- 22 V. C. Tung, M. J. Allen, Y. Yang, R. B. Kaner, *Nat Nanotechnol*, 2008, **4**, 25.
- 23 X. Du, I. Skachko, A. Barker, E. Y. Andrei, *Nat Nanotechnol*, 2008, **3**, 491.
- 24 J. S. Lee, K. H. You, C. B. Park, *Adv Mater*, 2012, **24**, 1084.
- 25 L. Zhang, H. Z. Li, Y. Liu, Z. Tian, B. Yang, Z. B. Sun, S. Q. Yan, *Rsc Adv*, 2014, **4**, 48703.
- 26 N. P. Herring, S. H. Olson, C. R. Almahoudi, M. S. El-Shall, *J Nanopart Res*, 2012, **14**, 1277.
- 27 M. Keerthi Vanitha, S. Vadivel, N. Balasubramanian, *Desalin Water Treat*, 2015, **54**, 2748.
- 28 W. Lu, J. Chen, Y. Wu, L. F. Duan, Y. Yang, X. Ge, *Nanoscale Res Lett*, 2014, **9**, 148.
- 29 M. Saranya, R. Ramachandran, P. Kollu, S. K. Jeong, A. N. Grace, *Rsc Adv*, 2015, **5**, 15831.
- 30 S. C. Yan, Z. S. Li, Z. G. Zou, *Langmuir* 2010, **26**, 3894.
- 31 Y. Cui, D. Zhou, Z. Y. Sui, B. H. Han, *Chinese J Chem*, 2015, **33**, 119.
- 32 Y. S. Yuan, X. Xu, Q. L. Zou, F. Y. Ji, Fan, Z. H. Zhou, *International Conference on Energy, Environment and Materials Engineering (Eeme 2014)*, 2014, **448**.
- 33 J. Hass, F. Varchon, J. E. Millán-Otoya, M. Sprinkle, N. Sharma, W. A. de Heer, C. Berger, P. N. First, L. Magaud, E. H. Conrad, *Phys Rev Lett*, 2008, **100**, 125504.
- 34 J. Hass, W. A. de Heer, E. H. Conrad, *Journal of Physics: Condensed Matter*, 2008, **20**, 323202.
- 35 K. V. Kumar, K. Porkodi, F. Rocha, *Catal Commun* 2008, **9**, 82.
- 36 Z. Xiong, L. L. Zhang, X. S. Zhao, *Chemistry - A European Journal*, 2011, **17**, 2428.
- 37 L.-W. Zhang, H.-B. Fu, Y.-F. Zhu, *Adv Funct Mater*, 2008, **18**, 2180.
- 38 J. M. Yun, J. S. Yeo, J. H. Kim, H. G. Jeong, D. Y. Kim, Y. J. Noh, S. S. Kim, B. C. Ku, S. I. Na, *Adv Mater* 2011, **23**, 4923.
- 39 D. Yang, L. Y. Zhou, L. C. Chen, B. Zhao, J. Zhang, C. Li, *Chem Comm* 2012, **48**, 8078.
- 40 J. Jiang, K. Zhao, X. Y. Xiao, L. Z. Zhang, *J Am Chem Soc*, 2012, **134**, 4473.
- 41 K. Hashimoto, M. Hiramoto, T. Sakata, *Chem Phys Lett*, 1988, **148**, 215.
- 42 T. X. Wu, G. M. Liu, J. C. Zhao, H. Hidaka, N. Serpone, *J Phys Chem B*, 1998, **102**, 5845.